Resveratrol Improves Oxidative Stress and Protects Against Diabetic Nephropathy Through Normalization of Mn-SOD Dysfunction in AMPK/SIRT1-Independent Pathway

Munehiro Kitada,[1] Shinji Kume,[2] Noriko Imaizumi,[1] and Daisuke Koya[1]

OBJECTIVE—Despite the beneficial effects of resveratrol (RSV) on cardiovascular disease and life span, its effects on type 2 diabetic nephropathy remain unknown. This study examined the renoprotective effects of RSV in *db/db* mice, a model of type 2 diabetes.

RESEARCH DESIGN AND METHODS—*db/db* mice were treated with RSV (0.3% mixed in chow) for 8 weeks. We measured urinary albumin excretion (UAE), histological changes (including mesangial expansion, fibronectin accumulation, and macrophage infiltration), oxidative stress markers (urinary excretion and mitochondrial content of 8-hydroxy-2'-deoxyguanosine [8-OHdG], nitrotyrosine expression), and manganese-superoxide dismutase (Mn-SOD) activity together with its tyrosine-nitrated modification and mitochondrial biogenesis in the kidney. Blood glucose, glycated hemoglobin, and plasma lipid profiles were also measured. The phosphorylation of 5′-AMP–activated kinase (AMPK) and expression of silent information regulator 1 (SIRT1) in the kidney were assessed by immunoblotting.

RESULTS—RSV significantly reduced UAE and attenuated renal pathological changes in *db/db* mice. Mitochondrial oxidative stress and biogenesis were enhanced in *db/db* mice; however, Mn-SOD activity was reduced through increased tyrosine-nitrated modification. RSV ameliorated such alterations and partially improved blood glucose, glycated hemoglobin, and abnormal lipid profile in *db/db* mice. Activation of AMPK was decreased in the kidney of *db/db* mice compared with *db/m* mice. RSV neither modified AMPK activation nor SIRT1 expression in the kidney.

CONCLUSIONS—RSV ameliorates renal injury and enhanced mitochondrial biogenesis with Mn-SOD dysfunction in the kidney of *db/db* mice, through improvement of oxidative stress via normalization of Mn-SOD function and glucose-lipid metabolism. RSV has antioxidative activities via AMPK/SIRT1-independent pathway. ***Diabetes*** **60:634–643, 2011**

Resveratrol (RSV; 3,5,4'-trihydroxystilbene) is reported to be beneficial in cardiovascular diseases (1) and renal diseases (2–4), including ischemic/reperfusion injury (5). The beneficial effects are thought to be due to its antioxidative properties because it is known as a robust scavenger of superoxide (O^{2-}), hydroxyl radicals, and peroxynitrite (6,7). Oxidative stress has been implicated in the pathogenesis of diabetic vascular complications, including nephropathy (8). The mitochondria are recognized as one of the major sources of reactive oxygen species (ROS) in diabetes (9), and they can also be damaged by ROS. Manganese-superoxide dismutase (Mn-SOD), which is an important antioxidative enzyme and mainly regulates ROS metabolism in the mitochondria, is one of the mitochondrial targets of ROS such as peroxynitrite, and thus its activity might become reduced with ROS exposure (10). Therefore, conditions that lead to Mn-SOD dysfunction could increase ROS production and hence induce tissue damage associated with diabetic nephropathy. However, it remains unclear whether mitochondrial oxidative stress associated with Mn-SOD dysfunction contributes to diabetes-induced renal injury, and whether RSV has any beneficial effects on mitochondrial status including oxidative stress and biogenesis in the kidney of type 2 diabetes.

Reduced mitochondrial biogenesis and function are found in insulin-resistant metabolic tissues including skeletal muscle, liver, and fat in association with the pathogenesis of type 2 diabetes (11). In addition to the scavenging of ROS, RSV enhances mitochondrial biogenesis through the 5′-AMP–activated kinase (AMPK)/silent information regulator 1 (SIRT1) pathway in the muscle and liver, resulting in life span extension or improvement of high-fat diet–induced metabolic impairment such as obesity and insulin resistance (12–14). On the other hand, mitochondrial biogenesis can be induced in tissues not only by increased energy demands due to cold, exercise, and metabolic changes such as those induced by caloric restriction (15), but also by damage to mitochondria caused by oxidative stress (16–18) and hereditary disorders (19). Oxidative stress-induced mitochondrial biogenesis has also been reported in various tissues and cells (16–18), including the myocardium of an animal model of type 1 diabetes (20). There is little information on whether mitochondrial status including mitochondrial biogenesis is changed in the kidney of type 2 diabetes, and if so, how it is regulated and whether it is related to the pathogenesis of diabetic nephropathy.

Thus, the aim of this study was to investigate the potential effects of RSV on mitochondrial oxidative stress associated with Mn-SOD dysfunction and mitochondrial biogenesis in the kidney of *db/db* mice. The results of the current study indicate that the enhanced mitochondrial biogenesis with Mn-SOD dysfunction induced by tyrosine nitration was observed in the diabetic kidney. Treatment with RSV resulted in the amelioration of these functional

From the [1]Division of Diabetes and Endocrinology, Kanazawa Medical University, Kahoku-Gun, Ishikawa, Japan; and the [2]Department of Medicine, Shiga University of Medical Science, Otsu, Shiga, Japan.
Corresponding author: Daisuke Koya, koya0516@kanazawa-med.ac.jp.
Received 19 March 2010 and accepted 1 December 2010.
DOI: 10.2337/db10-0386
This article contains Supplementary Data online at http://diabetes.diabetesjournals.org/lookup/suppl/doi:10.2337/db10-0386/-/DC1.

TABLE 1
Effects of RSV treatment on body weight, kidney weight, blood pressure, blood glucose, glycated hemoglobin, and lipid profiles in the four groups of mice. Glycated hemoglobin was measured using an ADAMS-HA8106 analyzer (ARKRAY, Kyoto, Japan). Serum insulin levels and urinary albumin excretion were measured with ELISA kits. Triglycerides, total cholesterol, and nonesterified fatty acid (NEFA) were measured using an L-type triglyceride H kit, cholesterol E-test kit, and NEFA C-test kit, respectively

	db/m	*db/m*+RSV	*db/db*	*db/db*+RSV
n	19	17	19	18
Body weight (g)	29.0 ± 2.31	28.6 ± 1.32	49.3 ± 2.70†	48.7 ± 1.92†
Right kidney weight (g)	0.196 ± 0.021	0.187 ± 0.012	0.233 ± 0.012†	0.217 ± 0.012‡§
Mean blood pressure (mmHg)	94.7 ± 5.30	94.9 ± 4.97	102.8 ± 6.56†	100.5 ± 5.18‖
Fasting blood glucose (mg/dL)	92.75 ± 4.18	90.63 ± 5.76	314.63 ± 50.72†	264.75 ± 44.17 †¶
Fasting serum insulin (ng/mL)	2.81 ± 1.54	2.88 ± 0.65	8.21 ± 3.59†	4.40 ± 1.44 †, #
*Random-fed blood glucose (mg/dL)	121.4 ± 28.50	117.6 ± 29.36	503.4 ± 64.80†	426.9 ± 90.52 †, **
Glycated hemoglobin (%)	3.66 ± 0.36	3.73 ± 0.31	8.7 ± 1.08†	7.78 ± 0.46 †, ††
Total cholesterol (mg/dL)	60.9 ± 8.12	62.2 ± 7.29	122.2 ± 22.84†	124.0 ± 22.03†
Triglyceride (mg/dL)	71.9 ± 20.9	65.4 ± 22.0	205.3 ± 52.10††	126.6 ± 58.07‡‡
Free fatty acids (mEq/L)	0.48 ± 0.128	0.48 ± 0.114	1.165 ± 0.275††	0.954 ± 0.196††
Urinary albumin excretion (μg/day)	44.56 ± 21.62	34.74 ± 20.37	382.99 ± 159.02††	189.00 ± 67.87‡‡

Data are means ± SD. *Random-fed blood glucose levels were measured at 9–10 A.M. †$P < 0.001$ vs. *db/m*, *db/m*+RSV. ‡$P < 0.05$ vs. *db/m*, *db/db*. §$P < 0.001$ vs. *db/m*+RSV. ‖$P < 0.05$ vs. *db/m*, *db/m*+RSV. ¶$P < 0.05$ vs. *db/db*. #$P < 0.01$ vs. *db/db*. **$P < 0.001$ vs. *db/db*. ††$P < 0.001$ vs. others, *db/db*. ‡‡$P < 0.01$ vs. *db/m*, *db/m*+RSV.

and histological abnormalities and mitochondrial biogenesis in the diabetic kidney, possibly by the attenuation of oxidative stress through scavenging of ROS, normalization of Mn-SOD dysfunction in an AMPK/SIRT1-independent mechanism, and partial improvement of glucose-lipid metabolism.

RESEARCH DESIGN AND METHODS

Materials and antibodies. Details of the materials and antibodies used in the current study are available in the Supplementary Data.

Animals. Male *db/db* mice and age-matched *db/m* mice were purchased from Clea Japan (Tokyo, Japan). At 9 weeks of age, mice were divided into four groups: *db/m* mice, *db/db* mice, *db/m* mice treated with RSV, and *db/db* mice treated with RSV. RSV was mixed (0.3%) with chow and administered orally. Body weight, blood glucose level, food consumption, and blood pressure were measured every 2 weeks in all animals. The blood pressure of conscious mice was measured at steady state by a programmable tail-cuff sphygmomanometer (BP98-A; Softron, Tokyo, Japan). At 17 weeks of age, individual mice were placed in metabolic cages for 24-h urine collection. The urine samples were stored at −80°C until analysis. Mice were anesthetized by intraperitoneal injection of pentobarbital sodium, and then the right kidneys were removed and stored at –80°C for experiments as described below. After collection of blood samples from the left cardiac ventricle, the left kidney was perfused with ice-cold phosphate-buffered saline (PBS) and 10% neutral buffered formalin and then removed. The Research Center for Animal Life Science of Kanazawa Medical University approved all experiments.

Morphological analysis and immunohistochemistry. To assess the mesangial expansion, thirty glomeruli, cut at the vascular pole, randomly selected from each mouse were measured the periodic acid/Schiff (PAS)-positive material in the mesangial area and glomerular tuft area by computer-assisted color image analysis (Micro Analyzer; Japan Poladigital, Tokyo, Japan) as previously described (21).

For semiquantitative evaluation of the fibronectin, F4/80 and nitrotyrosine scores, 20 randomly selected glomerulus or tubulointerstitial areas per mouse were graded in a double-blind manner, as reported previously (21–23), with minor modifications.

8-OHdG levels in mitochondrial DNA and quantification of mitochondrial DNA deletion mutation. The mitochondrial DNA (mtDNA) was extracted from the kidney using the mtDNA Extractor CT kit. The 8-OHdG levels in DNase I-digested mtDNA were determined by ELISA using a kit (8-OHdG Check, Institute for the Control of Aging, Shizuoka, Japan) (24). We determined. the deletion mutation, D-17, as reported previously (23). The sequences of primers are listed in Supplementary Table 1.

Detection of O^{2-} formation in renal isolated mitochondria. The mitochondria were isolated from the renal cortex of all groups of mice using the mitochondria isolation kit, according to the manufacturer's instructions. O^{2-} production from the mitochondria was measured by L-012 chemiluminescence (CL) dye (25). Mitochondrial suspensions were diluted to a final protein concentration of 0.1 mg/mL in 0.2 mL of PBS buffer containing 100 μmol/L L-012. O^{2-} from mitochondria was detected after stimulation with 4 mmol/L succinate and 20 μg/mL antimycin A by L-012. The CL registered at intervals of 30 s over 5 min with a chemiluminometer, and the signal was expressed as counts of CL/min/100 μg protein at 5 min. In ex vivo study, similar experiments were performed in isolated mitochondria from the renal cortex of *db/db* mice at various concentrations (10^{-3}–100 μmol/L) of RSV or 100 U/mL SOD. In addition, O^{2-} from the reaction of hypoxanthine and xanthine oxidase was also measured. L-012 (100 μM) was incubated for 5 min in PBS buffer containing 100 μmol/L diethylenetriamine pentaacetic acid (DTPA) and 1 mmol/L hypoxanthine at room temperature, and then the basal (background) signal was determined in a chemiluminometer at intervals of 30 s for 5 min. The CL was counted after the addition of 10 mU/mL xanthine oxidase at various concentrations of RSV (10^{-3}–100 μmol/L) or 100 U/mL SOD at intervals of 30 s over 5 min.

Mn-SOD activity. The whole kidney was homogenized in 2 mL of 50 mmol/L Tris HCl buffer containing 0.1 mmol/L ethylenediaminetetraacetic acid (EDTA) at pH 7.0. After centrifugation at 15,000*g* for 15 min, the supernatant was removed and total protein concentration was measured using a protein assay kit. The Mn-SOD activity was measured by inhibiting extracellular and cytosolic Cu/Zn SOD activity with KCN (1 mmol/L) using an SOD assay kit (WST-1) (26). One unit of SOD activity was defined as the amount causing 50% inhibition of the initial rate of reduction of WST-1 (2-(4-Iodophenyl)-3-(4-nitrophenyl)-5-(2, 4-disulfophenyl)-2H-tetrazolium, monosodium salt), a highly water-soluble tetrazolium salt. Mn-SOD activity was calculated in terms of protein content (U/μg) and expressed as a fold increase relative to that found in *db/m* mice.

Immunoprecipitation and Western blot analysis. The whole kidney was homogenized in ice-cold radioimmunoprecipitation assay (RIPA) buffer. Solubilized protein (1 mg) was used for immunoprecipitation with rabbit polyclonal anti–Mn-SOD antibody (10 μg/mL) using protein A-Sepharose, and then Western blot analysis was performed with mouse monoclonal antinitrotyrosine antibody (1:1000) or rabbit polyclonal anti–Mn-SOD antibody (1:1000). Samples of protein solutions from the kidney were used for Western blotting with antiphospho-AMPKα (Thr172) antibody, anti-AMPKα (23A3) antibody (1:1000), or anti-SIRT1 antibody (1:1000).

Quantitative real-time PCR. Isolation of total RNA from kidney, and determination of complementary DNA synthesis by reverse transcription and quantitative real-time PCR were performed as described previously (23). PCR primer sets are listed (Supplementary Table 1).

Cell culture. Murine proximal tubular cells (mProx) (derivative, patent WO9927363, Japan, U.S., European Union), kindly provided by CMIC Co., were cultured as described previously (27).

Retroviral infection. The pSUPERretro and pSUPERretro-SIRT1 RNA interference vectors were kind gifts from Dr. L. Guarente (Massachusetts Institute of Technology, Cambridge, MA). Human embryonic kidney 293T cells were transfected with pSUPERretro or pSUPERretro-SIRT1 RNAi by using Lipofectamine reagent. At 48 h after transfection, the media containing the retroviruses were collected, centrifuged, and transferred to mProx treated by

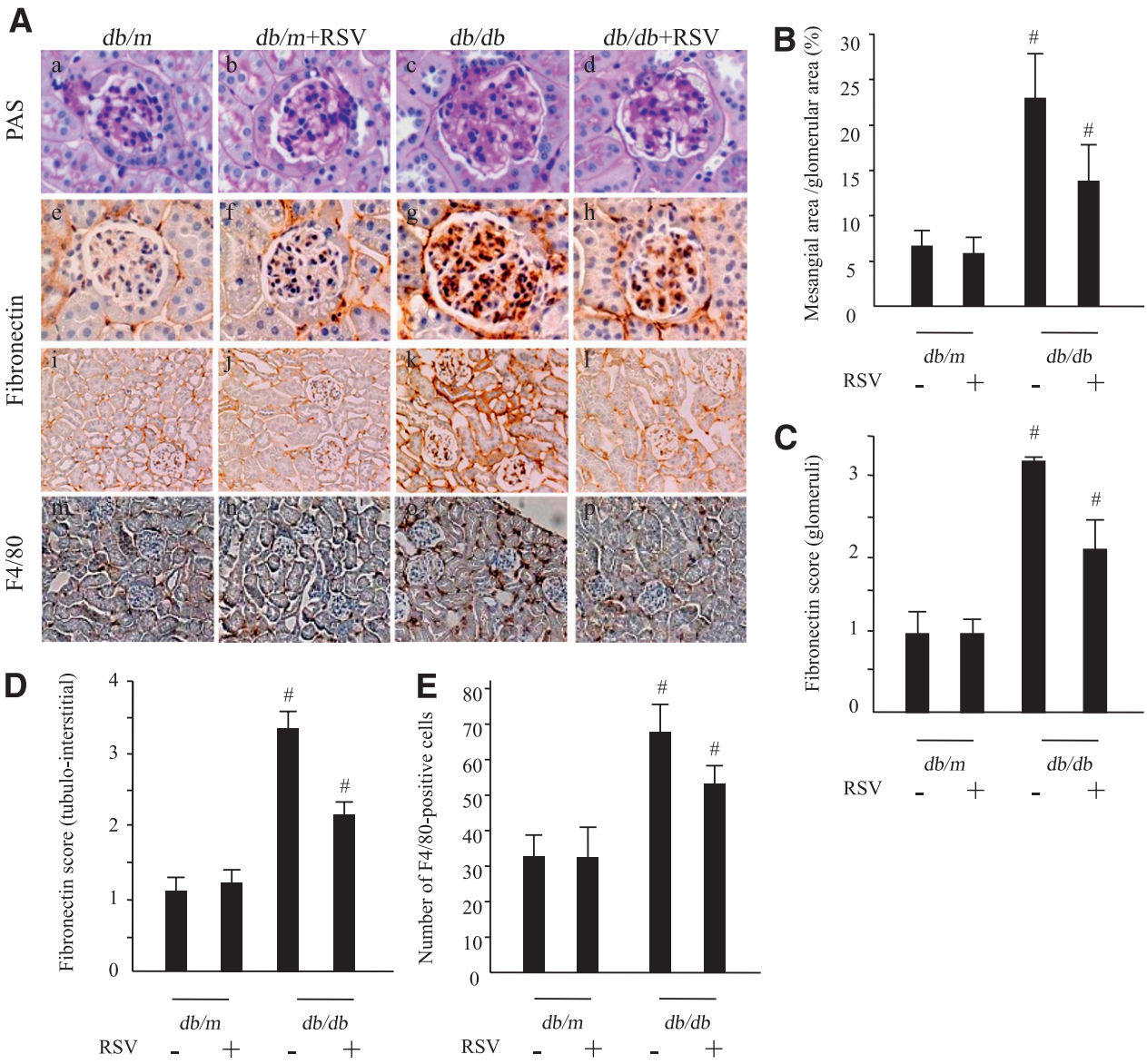

FIG. 1. Treatment with RSV ameliorates the mesangial matrix expansion in *db/db* mice. *A*: Representative photomicrographs of PAS-stained kidney (a–d). Data are results of independent experiments in each group with six mice per group. Original magnification: ×400. Treatment with RSV reduced glomerular and interstitial fibronectin accumulation and the number of F4/80-positive cells in *db/db* mice. Representative photomicrographs of immunohistochemistry for glomerular fibronectin (e–h), interstitial fibronectin (i–l), and F4/80 (m–p). Data are the results of independent experiments in each group with three to five mice per group. Original magnification, ×400 for glomerular fibronectin, ×200 for interstitial fibronectin, and ×100 for F4/80 staining. *B*: Quantitative assessment of the mesangial matrix area. Data are means ± SD (n = 6, #P < 0.01 vs. other groups). *C–E*: Quantitative assessment of fibronectin and F4/80 staining. Data are means ± SD (n = 3–5, #P < 0.01 vs. other groups). (A high-quality digital representation of this figure is available in the online issue.)

polybrene (1 g/mL). The infected cells were selected by treatment with puromycin (2.5 μg/mL) for several days as described previously (28).

Infection of adenoviral dominant negative-AMPK. Adenoviruses containing green fluorescent protein (Ad-GFP) or dominant-negative AMPK (DN-AMPK) were added to subconfluent mProx at a concentration of 50 multiplicity of infection for 1 h at 37°C in serum-free Dulbecco's modified Eagle's medium (29).

Detection of ROS in mProx. To determine the effect of RSV on oxidative stress in mProx, cells were incubated with RSV (10 μmol/L) for 180 min at 37°C before exposure to H_2O_2 (10 μmol/L). After incubation, the levels of intracellular ROS were measured with the fluoroprobe 2.7-dichlorodihydrofluorescein diacetate. The intracellular ROS was evaluated as the fluorescence intensity (an excitation wavelength 488 nm, an emission wavelength 525 nm) of dichlorofluorescein by Infinite M200 microplate reader (Tecan Japan Co., Kanagawa, Japan). The results of intracellular ROS are expressed in arbitrary units.

mtDNA content. Well-conserved nuclear and other mitochondrial genes were selected to quantify mtDNA copy number per nuclear genome. Cytochrome *c* oxidase subunit 2 was used as a marker for mtDNA and uncoupling protein 2 for nuclear DNA. Renal DNA was extracted from frozen kidney tissues of all animals using the DNeasy tissue kit. Total DNA concentration was determined using a PicoGreen DNA quantitation kit. Specific mouse primer sequences are provided in the Supplementary Table 1. mtDNA per nuclear genome was calculated as the ratio of cytochrome *c* oxidase subunit 2 DNA to uncoupling protein 2 DNA (30) and expressed as the fold increase relative to that found in *db/m* mice.

Citrate synthase activity. Citrate synthase activity in the kidney was determined using the citrate synthase activity measurement kit, according to the manufacturer's instructions.

Electron microscopy. The mitochondria in proximal tubular cells were observed by electron microscopy as previously described (23). Mitochondrial area and number were estimated in 15–18 micrographs, which were taken for renal proximal tubular cells of three animals of each group (20). The mitochondrial area was measured using the ImageJ software, and the number of mitochondria per cell was counted manually by a blind observer.

Statistical analysis. Data are expressed as means ± SD. The Tukey multiple-comparison test was used to determine the significance of pairwise differences among three or more groups. $P < 0.05$ was considered significant.

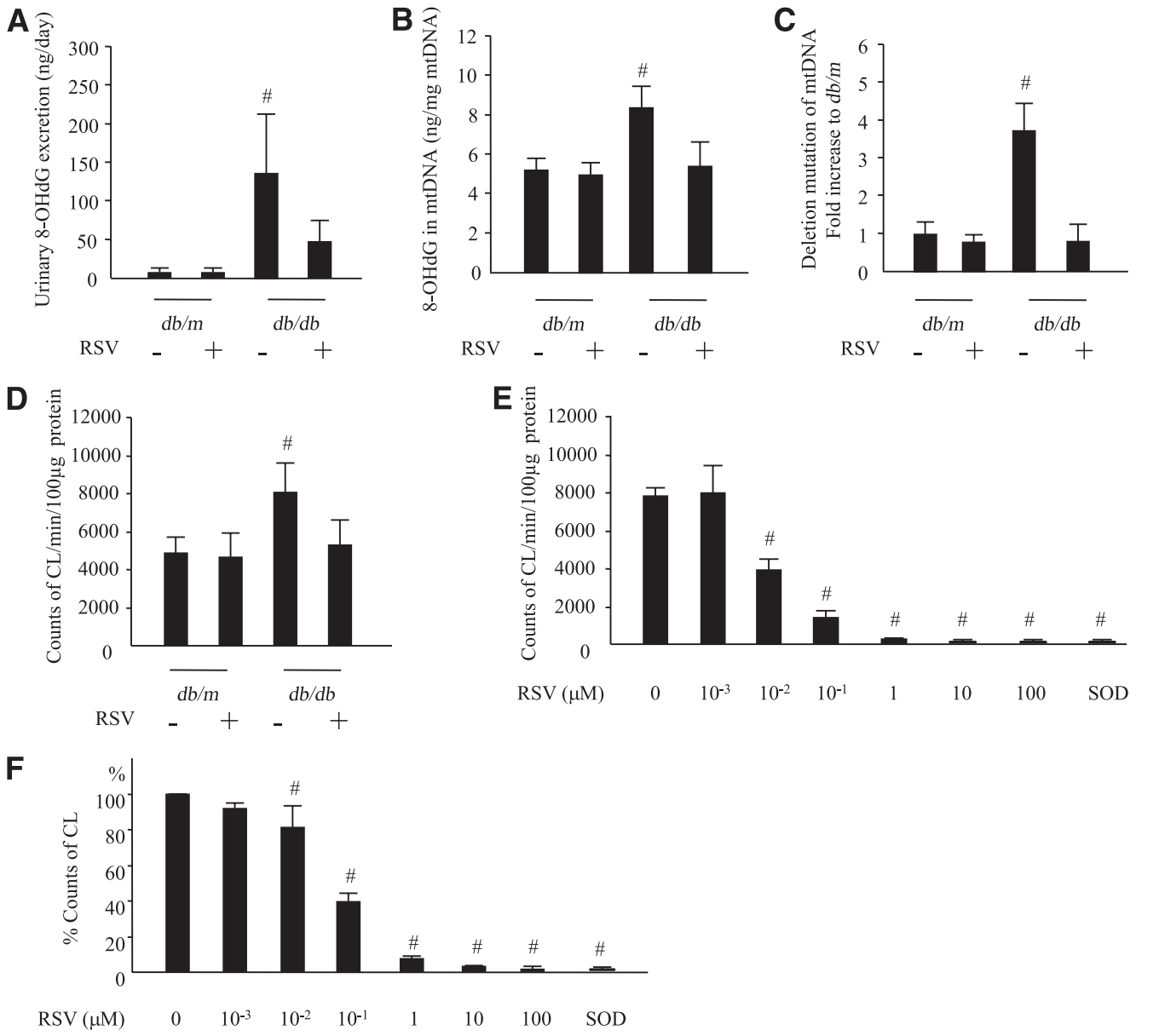

FIG. 2. RSV suppresses oxidative damage in *db/db* mice, and RSV scavenges O^{2-} production from mitochondria. *A*: Urinary 8-OHdG excretion for 24 h was measured. Data are means ± SD (n = 9–11, #P < 0.05 vs. other groups). *B*: 8-OHdG contents in mtDNA of the kidney samples were measured. Data are means ± SD (n = 3–4, #P < 0.05 vs. *db/m* mice group). *C*: Frequencies of deletion mutation of mtDNA in the kidney were determined by quantitative PCR method. Data are means ± SD (n = 3–4, #P < 0.05 vs. other groups). *D*: O^{2-} production from renal isolated mitochondria by stimulation with succinate and antimycin A was determined in all groups. O^{2-} production was expressed as counts of CL per 100 μg protein. Data are means ± SD (n = 8, #P < 0.05 vs. *db/m* mice group). *E*: O^{2-} production in mitochondria isolated from the kidneys of *db/db* mice by stimulation with succinate and antimycin A was measured in RSV at various concentrations (10^{-3}–100 μmol/L) or SOD (100 U/mL). O^{2-} production was expressed as counts of CL per 100 μg protein. Data are means ± SD (n = 8, #P < 0.01 vs. control [0]). *F*: O^{2-} production from the reaction of hypoxanthine/xanthine oxidase was measured in RSV at various concentrations (10^{-3}–100 μmol/L) or SOD (100 U/mL). The inhibitory effect of RSV against O^{2-} on this reaction was expressed as % counts of CL. Data are means ± SD (n = 4, #P < 0.01 vs. control [0]).

RESULTS

Characteristics of experimental mice. Table 1 details the characteristics of four groups of mice at the end of the experimental period. The whole body and right kidney weights were significantly higher in *db/db* mice compared with *db/m* mice. The mean blood pressure (MBP) was significantly higher in *db/db* mice than in *db/m* mice. RSV did not affect changes in MBP. *db/db* mice exhibited markedly elevated blood glucose levels compared with *db/m* mice throughout the entire experiment. In *db/db* mice, treatment with RSV induced a partial improvement in blood glucose levels and glycated hemoglobin by the end of the experiments. Serum lipid profiles including total cholesterol, triglyceride, and free fatty acid levels were also significantly elevated in *db/db* mice compared with *db/m* mice; the increases in triglycerides and free fatty acids were partially rescued by RSV (Table 1). In addition, an impairment of glucose and insulin tolerance was evident in *db/db* mice relative to *db/m* mice (Supplementary Fig. 1), and high levels of fasting glucose and insulin (Table 1) indicating insulin resistance were also observed in *db/db* mice. Such alteration of insulin resistance in *db/db* mice was partially improved by treatment with RSV. There were no differences in body weight and food consumption between

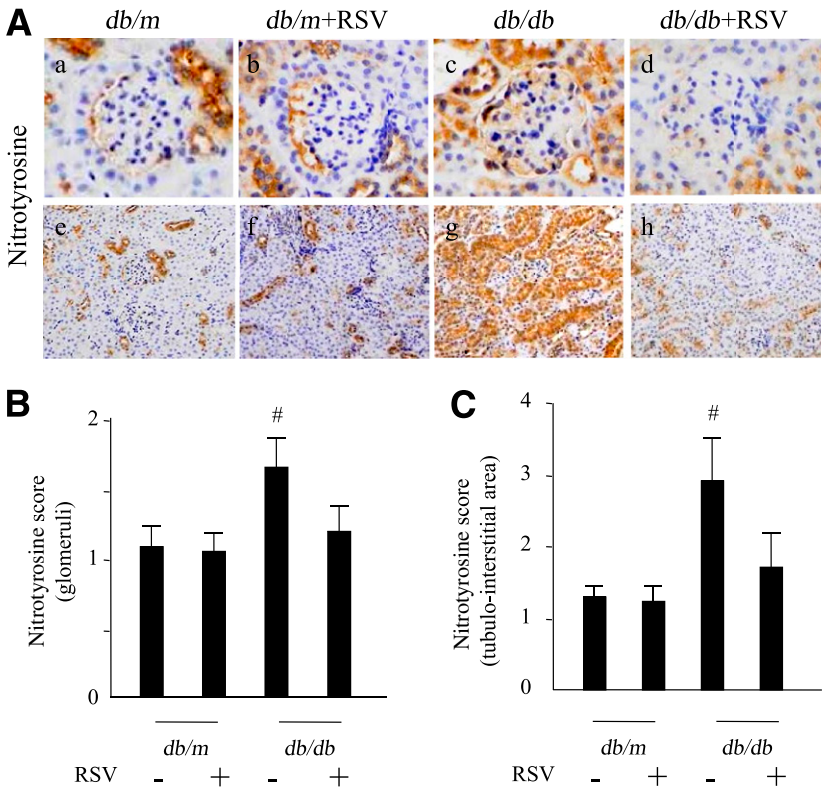

FIG. 3. Treatment with RSV suppresses diabetes-induced nitrotyrosine staining in the mouse kidney. *A*: Representative photomicrographs of renal nitrotyrosine expression. Data are results of independent experiments in each group with six mice per group. Original magnification: ×400 for glomerular nitrotyrosine (a–d) and ×100 for tubulointerstitial nitrotyrosine (e–h) staining. *B* and *C*: Semiquantitative scores for nitrotyrosine in glomerular and tubulointerstitial lesions. Data are means ± SD (n = 6, #P < 0.05 vs. other groups). (A high-quality digital representation of this figure is available in the online issue.)

untreated and RSV-treated *db/db* mice. The 24-h urine volume was significantly larger in *db/db* mice compared with *db/m* mice, and this was partially reduced by treatment with RSV (data not shown).

Changes in urinary albumin excretion. To evaluate the effects of RSV on functional abnormalities in *db/db* mice, we measured the urinary albumin excretion. Values were markedly higher in *db/db* mice and RSV treatment significantly reduced urinary albumin excretion (Table 1), indicating that RSV ameliorates the functional abnormality of diabetic nephropathy in *db/db* mice.

Changes in kidney morphology. Figure 1*A* a–d shows representative photomicrographs of mesangial matrix accumulation in the PAS-stained kidneys of the four groups. The mesangial matrix was more extensive in the glomeruli of *db/db* mice than in *db/m* mice, and treatment with RSV reduced such expansion. Figure 1*B* shows the results of quantitative analysis of mesangial matrix expansion in all groups. Although the ratio of mesangial matrix/glomerular area was markedly larger in *db/db* mice than in *db/m* mice, treatment with RSV significantly reduced this expansion.

Immunohistochemistry for fibronectin (Fig. 1*A* e–h and i–l) also showed a significantly higher score for renal glomerular and tubulointerstitial expression in *db/db* mice than in *db/m* mice (Fig. 1*C* and *D*). Treatment with RSV reduced the score for fibronectin in *db/db* mice but had no effect on *db/m* (Fig. 1*C* and *D*).

The number of cells positive for F4/80 (a macrophage marker) in the renal interstitial lesion was significantly higher in *db/db* mice than in *db/m* mice (Fig. 1*A* m–p), but this pattern was not found in the glomeruli (data not shown). Treatment with RSV reduced the number of F4/80-positive cells in the renal interstitial lesions of *db/db* mice (Fig. 1*E*). These results indicate that RSV might improve glomerular and interstitial histological abnormalities including mesangial expansion, fibronectin accumulation and increased interstitial macrophage infiltration in the kidney of *db/db* mice.

Changes in urinary 8-OHdG excretion and mitochondrial oxidative damage in the kidney. Urinary 8-OHdG excretion was markedly higher in *db/db* mice compared with *db/m* mice but diminished after treatment with RSV (Fig. 2*A*). The 8-OHdG content (Fig. 2*B*) and subsequent deletion mutation (Fig. 2*C*) in the mtDNA isolated from the kidneys of *db/db* mice were significantly higher than in *db/m* mice. These mitochondrial alterations in mtDNA were not observed in the kidney of *db/db* mice treated with RSV. In addition, O^{2-} production from the isolated renal mitochondria after stimulation with succinate and antimycin A was significantly increased in *db/db* mice, but treatment with RSV restored it to normal in *db/db* mice. In ex vivo experiments, the addition of RSV exogenously attenuated the levels of O^{2-} from the renal mitochondria of *db/db* mice in a dose-dependent manner (Fig. 2*D*). Moreover, RSV could also scavenge O^{2-} production from reaction of hypoxanthine and xanthine oxidase in a dose-dependent manner. These results suggest that the enhancement of both systemic oxidative damage and renal mitochondrial oxidative damage was observed in *db/db* mice and that RSV has antioxidative activity.

Changes in nitrotyrosine expression in the kidney. Figure 3*A* a–h show representative immunohistochemical staining for nitrotyrosine in the kidney. The semiquantitative

scores for nitrotyrosine in both the glomerular and the tubulointerstitial lesions of the renal cortex were increased in *db/db* mice compared with those of *db/m* mice (Fig. 3*B* and *C*). Treatment with RSV reduced the scores in the glomeruli and tubulointerstitium of *db/db* mice but had no effect on the lesions of *db/m* mice (Fig. 3*B* and *C*). These results indicate that tyrosine nitration of proteins is enhanced in the kidney of *db/db* mice and that RSV seems to attenuate the effect.

Changes in Mn-SOD expression and activity in the kidney. The mRNA and protein expression of Mn-SOD was higher in *db/db* mice than in *db/m* mice (Fig. 4*A*–*C*). The Mn-SOD activity was significantly lower in the kidney of *db/db* mice compared with that of *db/m* mice (Fig. 4*D*). Nitrotyrosine immunoreactivity was significantly higher in Mn-SOD immunoprecipitates from the kidney of *db/db* mice than in that from *db/m* mice, and the increase in immunoreactivity was attenuated by treatment with RSV in *db/db* but not *db/m* mice (Fig. 4*E* and *F*). These findings suggest that Mn-SOD activity could be reduced by modifying tyrosine nitration in the kidneys of *db/db* mice.

mRNA levels of mitochondrial biogenesis–related genes and the enzyme activity of citrate synthase. To evaluate mitochondrial biogenesis, we assessed peroxisome proliferator-activated receptor γ coactivator (PGC)-1α, nuclear respiratory factor (NRF)-1, and cytochrome c oxidoreductase mRNA expression levels and mtDNA contents in the kidney. The citrate synthase activity was also measured in the kidney. All these were significantly higher in the kidneys of *db/db* mice than in that of *db/m* mice (Fig. 5*A*–*E*). These changes improved following treatment with RSV, consistent with the observed normalization of Mn-SOD activity and oxidative stress.

Electron microscopy. To confirm the beneficial effects of RSV on mitochondrial biogenesis, we examined the renal morphology in more detail by electron microscopy. The number and area of the mitochondria were significantly larger in renal proximal tubular cells of *db/db* mice compared with *db/m* mice, but treatment with RSV rescued these differences in *db/db* mice (Fig. 6*A*–*C*).

Changes in AMPK activation and SIRT 1 expression in the kidney. We assessed whether RSV activates AMPK in the kidney using immunoblotting for phosphorylation of AMPK. Activation of AMPK was significantly reduced in the kidney of *db/db* mice compared with *db/m* mice, and RSV did not alter AMPK activation in the kidney (Fig. 7*A* and *B*). In addition, SIRT1 expression was no different among the groups (Fig. 7*A* and *C*).

RSV exerts antioxidative effects in AMPK/SIRT1-independent mechanism in cultured renal proximal tubular cells. RSV attenuated intracellular ROS in both the SIRT1-knocked-down and DN-AMPK–overexpressing

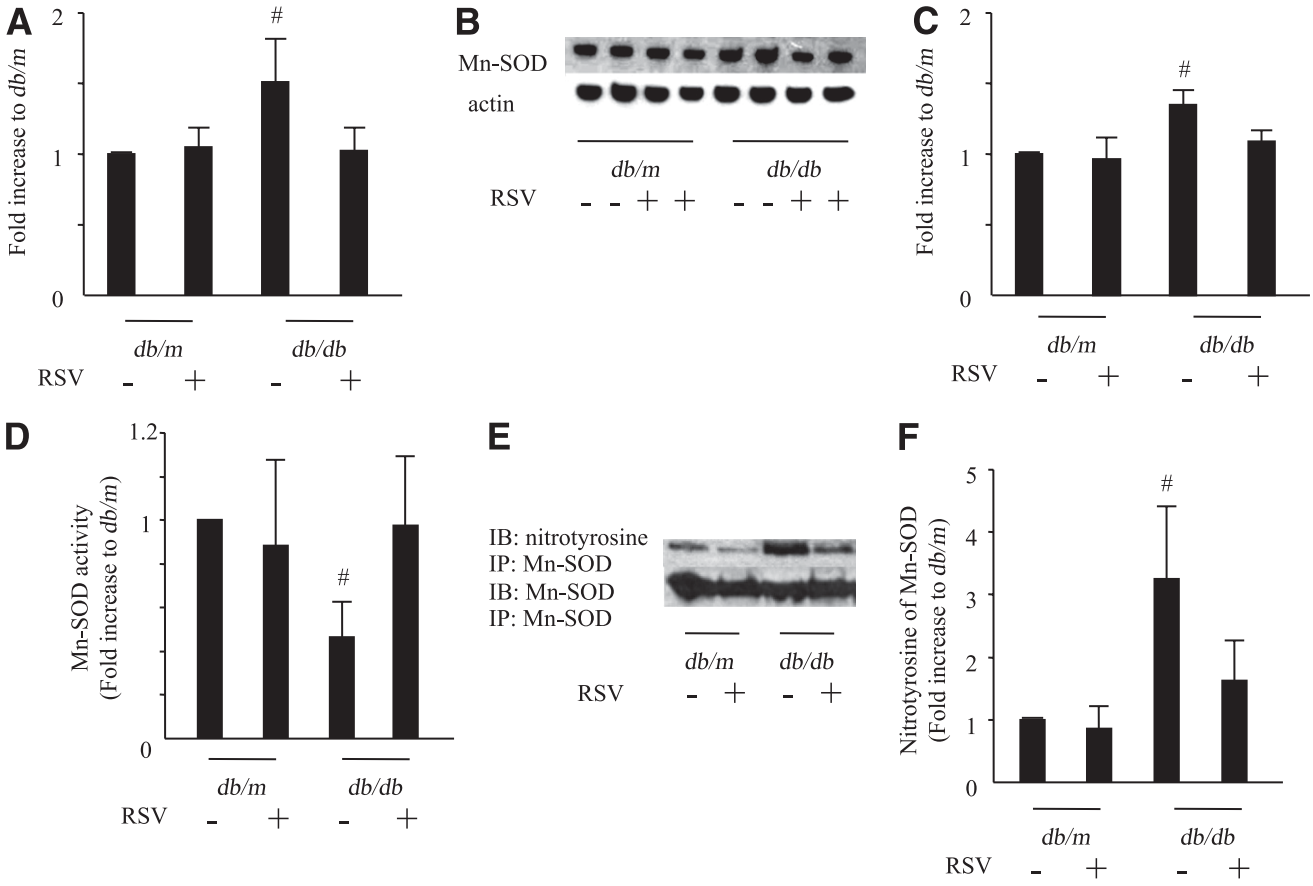

FIG. 4. Mn-SOD expression and activity in the kidney. *A*: Mn-SOD mRNA expression in kidneys was quantified by real-time PCR and expressed as fold increase relative to *db/m* mice. Data are means ± SD (n = 9–11, #P < 0.05 vs. other groups). *B*: Mn-SOD protein expression in the kidney shown by representative immunoblots of Mn-SOD in protein extracts from the kidneys of mice of each group. Actin was loaded as an internal control. *C*: Quantitative analysis of Mn-SOD protein expression in the kidneys. Data are means ± SD (n = 4, #P < 0.05 vs. other groups). *D*: Mn-SOD activity in the kidney homogenate is expressed as fold increase compared with *db/m* mice. Data are means ± SD (n = 9–11, #P < 0.05 vs. other groups). Immunoreactivity to nitrotyrosine for immunoprecipitated Mn-SOD. Proteins from the kidneys of each group were immunoprecipitated with anti–Mn-SOD antibodies and blotted for nitrotyrosine antibodies. Representative results of Western blotting are shown (*E*), and the ratio to immunoprecipitated Mn-SOD is shown (*F*). Data are means ± SD (n = 6, #P < 0.05 vs. other groups).

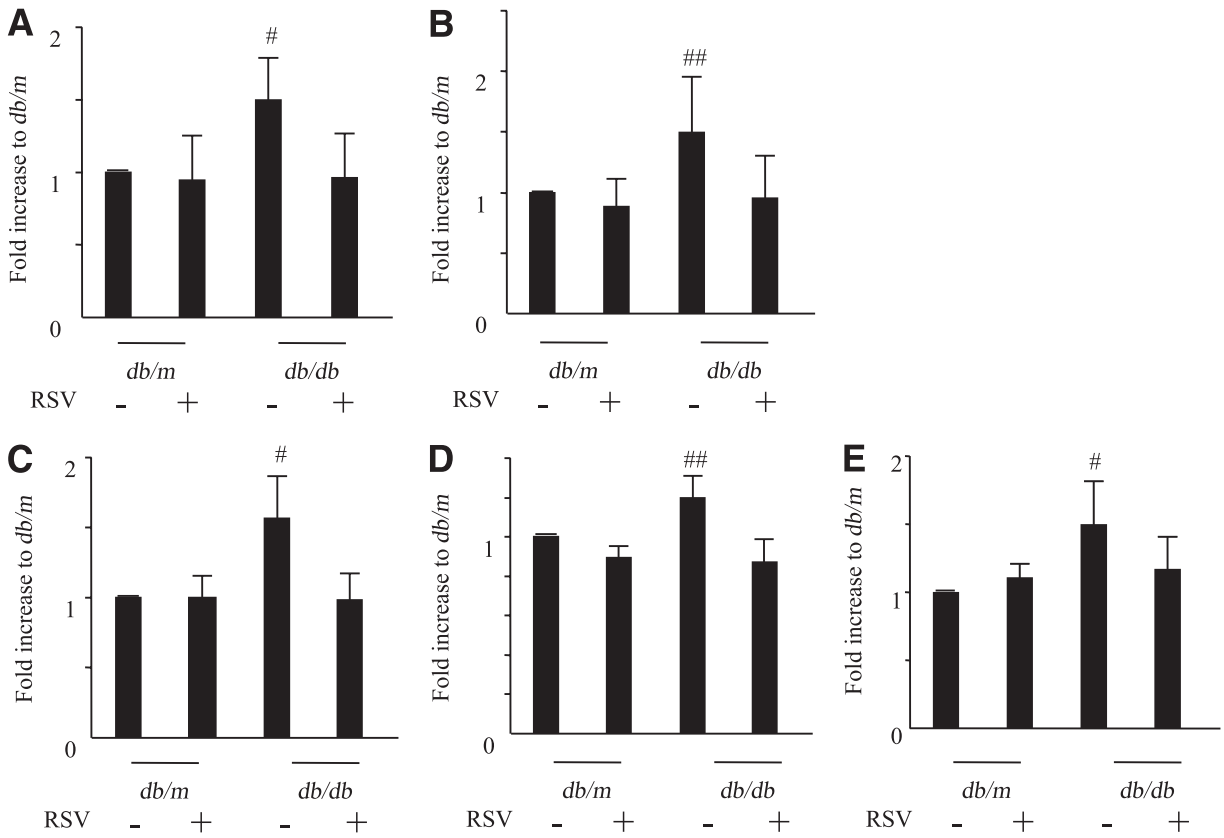

FIG. 5. PGC-1α, NRF-1, and cytochrome c oxidoreductase mRNA expression levels, mtDNA contents, and the enzyme activity of citrate synthase in the kidney. The mRNA expression levels of PGC-1α (*A*), NRF-1 (*B*), cytochrome c oxidoreductase (*C*), and mtDNA contents (*D*) were quantified by real-time PCR and expressed as fold increases from *db/m* mice. Data are means ± SD (*n* = 9–11, mRNA expression, *n* = 6–8; mtDNA content, #*P* < 0.05 vs. other groups, ##*P* < 0.01 vs. other groups). *E*: The citrate synthase activity was measured in the kidney of all groups. Data are means ± SD (*n* = 8, #*P* < 0.05 vs. other groups).

renal proximal tubular cells as well as in control cells. These results indicate that RSV exerts antioxidative effects independent of the AMPK/SIRT1 pathway (Fig. 7*D* and *E*).

DISCUSSION

In this study, we showed the potential benefits of RSV in ameliorating the renal injury and the enhanced mitochondrial biogenesis with Mn-SOD dysfunction observed in the diabetic kidney. We also demonstrated that RSV seems to exert these effects by improving the oxidative stress status in the kidney via the scavenging of ROS, normalization of Mn-SOD dysfunction, and partial rescue of glucose-lipid metabolism. Also, such antioxidative effects of RSV could be exerted in an AMPK/SIRT1-independent mechanism.

First, we showed that RSV improved renal functional and histological abnormalities such as albuminuria, mesangial expansion, glomerular and interstitial fibronectin accumulation, and interstitial macrophage infiltration in the kidney of *db/db* mice, a type 2 diabetes animal model. Oxidative stress has been implicated in the pathogenesis of diabetic nephropathy, and high glucose-induced ROS in renal mesangial or tubular cells contribute to overproduction of extracellular matrix proteins and inflammation (31,32). Because it has been reported that RSV is a robust scavenger of ROS (6,7), we assessed whether RSV has beneficial effects against diabetes-induced systemic and renal oxidative stress by measuring urinary 8-OHdG excretion and renal immunostaining for nitrotyrosine. Moreover, not only are mitochondria an important source of ROS, but also they themselves can be damaged by ROS. Therefore, we also assessed renal mitochondrial oxidative stress by measuring accumulation of mitochondrial 8-OHdG and D-17 deletion of mtDNA, which have been observed in diabetic nephropathy (33) and aging (24). In the current study, renal nitrotyrosine expression and mitochondrial oxidative damage indicated systemic, renal and particularly mitochondrial enhanced oxidative stress in the kidney of *db/db* mice, and there was clear attenuation of these markers following treatment with RSV. In addition, we showed that isolated mitochondrial O^{2-} production by stimulation with succinate and antimycin A was increased in *db/db* mice, and the RSV could scavenge ROS from the mitochondria.

The mitochondria are an important source of ROS in diabetes (9), and ROS metabolism in the mitochondria is mainly regulated by Mn-SOD, which is an important antioxidative enzyme in the mitochondria. In the diabetic state, high glucose- or FFA-induced overproduction of ROS from the mitochondria is inhibited by overexpression of Mn-SOD in vascular cells and tissues (9,34–37). Moreover, heterozygous Mn-SOD deficient mouse, which only have 50% of the Mn-SOD activity seen in wild-type mice, showed O^{2-}-induced mitochondrial oxidative damage (38), together with massive glomerulosclerosis, tubulointerstitial damage and inflammation including macrophage infiltration in the kidney (39). Therefore, regulation of ROS metabolism

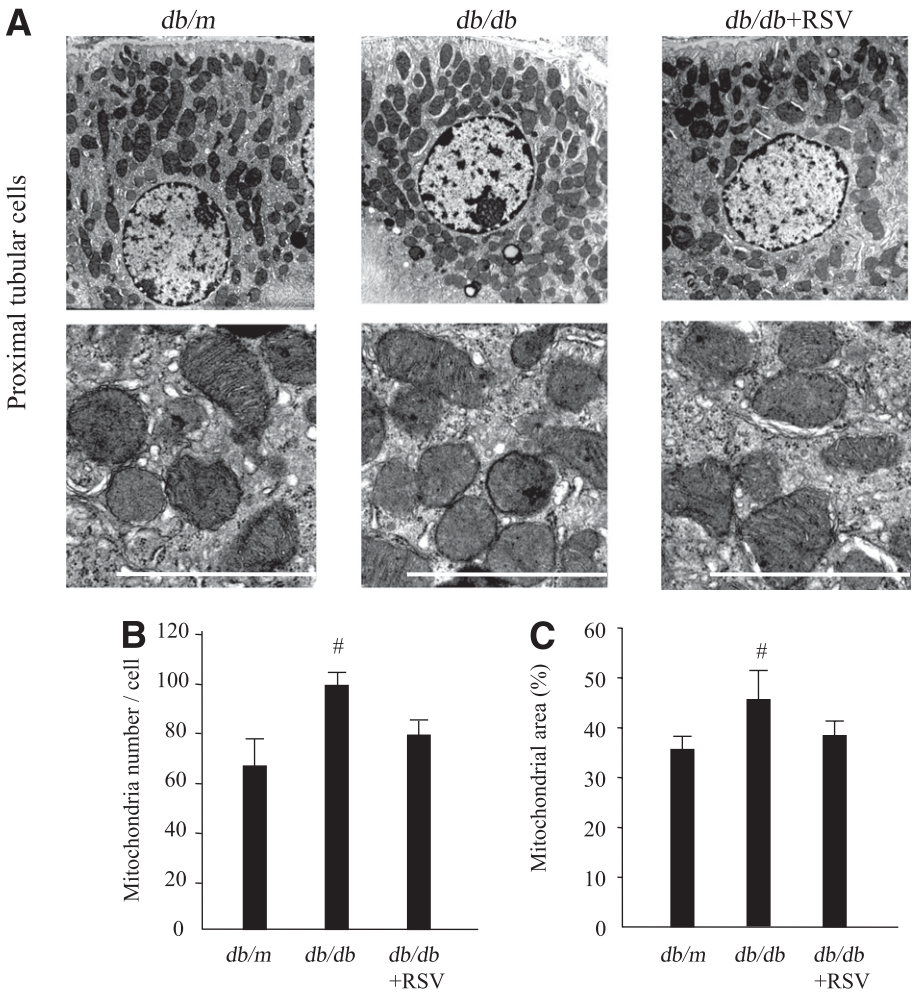

FIG. 6. Electron microscopy of kidney. *A*: Representative micrographs of proximal tubular cells from mice treated with RSV. Scale bar = 2 μm. Quantitative assessment of number (*B*) and area (*C*) of mitochondria in proximal tubular cells in mice treated with RSV. Data are means ± SD (n = 3, #P < 0.01 vs. other groups).

in the mitochondria via Mn-SOD function is an important protective factor in managing diabetic vascular complications including nephropathy. It is also known that tyrosine nitration at the active site of Mn-SOD is associated with reduction in enzymatic activity in the kidneys of several disease models (26,40–42). In the current study, we showed reduced Mn-SOD activity even when the expression of Mn-SOD was increased, and the former was probably caused by increased tyrosine nitration in the kidney of *db/db* mice. RSV might reduce tyrosine nitration of Mn-SOD and rescue the activation, resulting in improvement of mitochondrial oxidative stress and renal injury in diabetic kidney. Thus, RSV might ameliorate systemic, renal, and particularly mitochondrial oxidative stress in diabetes via the direct scavenging of ROS and normalization of the Mn-SOD function.

It has been reported recently that reduced mitochondrial biogenesis in insulin resistant tissues such as skeletal muscle, liver, or fat is associated with the pathogenesis of type 2 diabetes (11). In addition to its function as a ROS scavenger, several reports have implicated RSV in activating the AMPK/SIRT1 pathway to induce mitochondrial biogenesis (14), leading to life span prolongation and improvement of high-fat diet–induced metabolic impairment such as obesity and insulin resistance (12,13). We therefore examined mitochondrial biogenesis in the kidney based on mtDNA contents, mitochondria area and number, citrate synthase activity and overexpression of PGC-1α, NRF-1, cytochrome *c* oxidoreductase, and Mn-SOD. Interestingly, these factors were all enhanced in the kidney of *db/db* mice compared with *db/m* mice, and were rescued by RSV treatment, consistent with attenuation of systemic and renal mitochondrial oxidative stress including tyrosine nitration of Mn-SOD. Moreover, RSV did not alter AMPK activation or induction of Mn-SOD expression in the kidney. We also showed that RSV attenuated intracellular ROS in both the SIRT1 knocked-down and the DN-AMPK–overexpressing renal proximal tubular cells. These results suggest that systemic and/or renal mitochondrial oxidative stress contributes to the enhanced mitochondrial biogenesis in the kidney of the *db/db* mice and that RSV might improve mitochondrial biogenesis through the attenuation of oxidative stress, rather than through the activation of the AMPK/SIRT1 pathway. In this regard, Shen et al. (20) demonstrated that oxidative stress–induced mitochondrial biogenesis was increased in the myocardium of OVE26 diabetic mice as a possible compensatory reaction against oxidative stress–induced mitochondrial damage. Moreover, they showed that the myocardium-specific Mn-SOD transgenic mice crossed with OVE26 diabetic mice showed

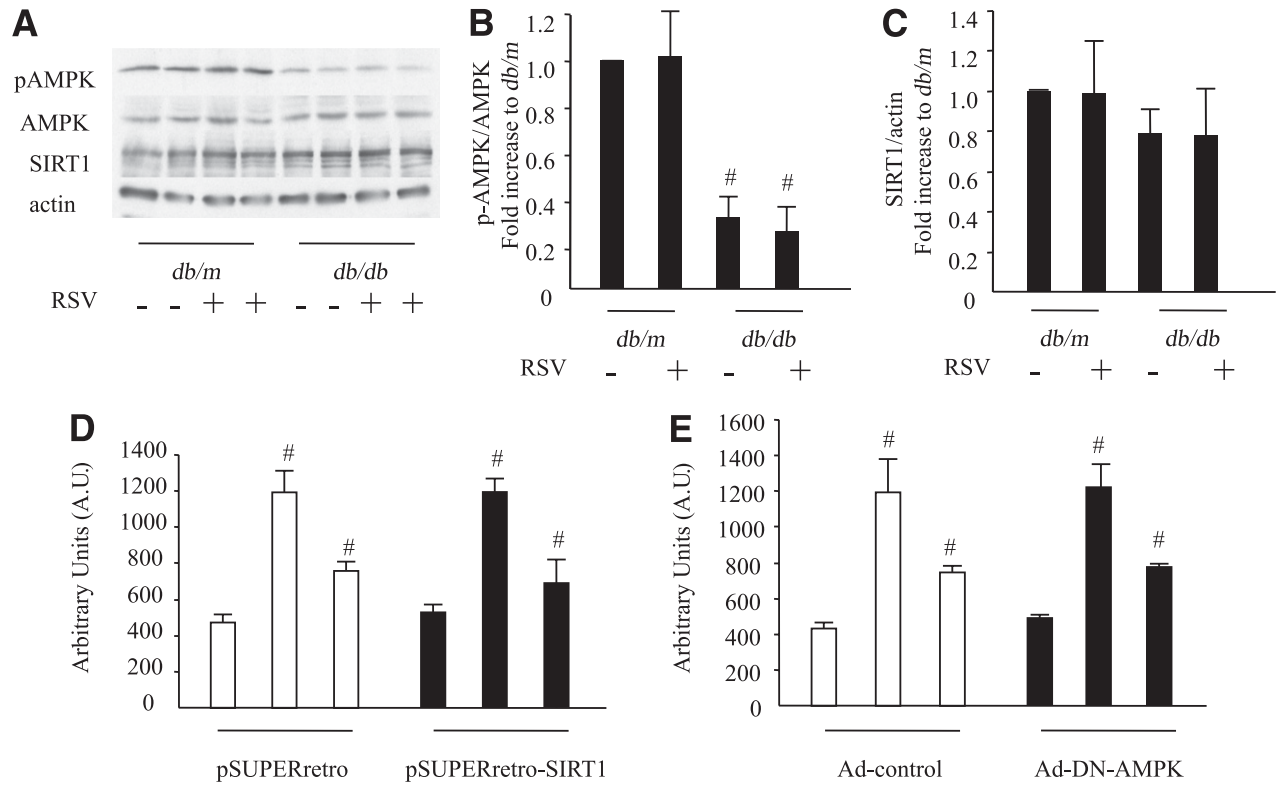

FIG. 7. AMPK activation and SIRT1 expression in the kidney and RSV attenuates ROS in both the SIRT1-knocked-down and the DN-AMPK–overexpressing renal mProx. *A*: Representative immunoblots of phospho-AMPKα (Thr172), AMPKα, and SIRT1 in protein extracts from the kidneys of mice of each group. Actin was loaded as an internal control. *B*: Quantitative analysis of phospho-AMPKα (Thr172). *C*: Quantitative analysis of SIRT1 protein expression. Data are means ± SD (n = 4, #P < 0.05 vs. *db/m* mice and *db/m* mice treated with RSV). *D*: Effects of RSV on the attenuation of oxidative stress in both the pSUPERretro and pSUPERretro-SIRT1 infected mProx exposed to H_2O_2. Data are means ± SD (n = 3, #P < 0.05 vs. other groups). *E*: Effects of RSV on the attenuation of oxidative stress in the adenovirus including GFP or DN-AMPK–overexpressing mProx exposed to H_2O_2. Data are means ± SD (n = 3, #P < 0.05 vs. other groups).

improvement of oxidant-induced mitochondrial biogenesis and dysfunction (37). Therefore, we suggest that the enhanced mitochondrial biogenesis in the kidney of *db/db* mice might also be a compensatory response to oxidative stress–induced mitochondrial damage; however further study is needed to elucidate the role of enhanced mitochondrial biogenesis associated with Mn-SOD dysfunction.

RSV has also been shown to reduce elevated blood glucose levels and metabolic impairment in diabetes, to be associated with mitochondrial biogenesis through the AMPK/SIRT1 activation pathway, as discussed above (12,13,43). In the current study, the elevated levels of glucose, glycated hemoglobin, triglycerides, and free fatty acids and impairment of glucose/insulin tolerance in *db/db* mice improved to some extent by treatment with RSV. It is therefore possible that RSV acts as an enhancer of mitochondrial biogenesis through AMPK/SIRT1 activation in liver and skeletal muscle, resulting in demonstrated improvements in abnormal glucose-lipid metabolism in *db/db* mice. In fact, we found that the phosphorylation of AMPK was reduced in the liver of *db/db* mice, and RSV could restore its alteration (data not shown). Therefore, RSV is likely exerting some of its effects via improvement of glucose homeostasis, and the systemic improvement of metabolism might at least in part contribute to the amelioration of renal oxidative stress and renal injury.

In conclusion, our study indicated that the enhanced mitochondrial biogenesis with Mn-SOD dysfunction by tyrosine nitration was observed in the diabetic kidney. RSV seems to improve these functional and histological abnormalities and ameliorate the enhanced mitochondrial biogenesis in diabetic kidney, possibly by attenuating the oxidative stress through scavenging of the ROS, by the normalization of the Mn-SOD dysfunction in an AMPK/SIRT1-independent mechanism, and by the partial improvement of the glucose and lipid metabolism.

ACKNOWLEDGMENTS

This work was supported by a Grant-in-Aid for Scientific Research (21591148) to D.K., and the grant from the Uehara Memorial Foundation to D.K.

No potential conflicts of interest relevant to this article were reported.

M.K. collected and analyzed the data and wrote the manuscript. S.K. collected and analyzed the data and contributed to discussion. N.I. collected and analyzed the data. D.K. contributed to discussion and reviewed and edited the manuscript.

The authors thank Yuki Tanaka and Eiko Kobori for the technical support on fibronectin immunohistochemistry and maintenance of animals and collecting their physiological data. The authors also thank Dr. Issa F.G., WordMedex Pty Ltd. for help with preparing the manuscript.

REFERENCES

1. Bradamante S, Barenghi L, Villa A. Cardiovascular protective effects of resveratrol. Cardiovasc Drug Rev 2004;22:169–188
2. Do Amaral CL, Francescato HD, Coimbra TM, et al. Resveratrol attenuates cisplatin-induced nephrotoxicity in rats. Arch Toxicol 2008;82:363–370

3. Nihei T, Miura Y, Yagasaki K. Inhibitory effect of resveratrol on proteinuria, hypoalbuminemia and hyperlipidemia in nephritic rats. Life Sci 2001;68:2845–2852
4. Sharma S, Anjaneyulu M, Kulkarni SK, Chopra K. Resveratrol, a polyphenolic phytoalexin, attenuates diabetic nephropathy in rats. Pharmacology 2006;76:69–75
5. Sener G, Tuğtepe H, Yüksel M, Cetinel S, Gedik N, Yeğen BC. Resveratrol improves ischemia/reperfusion-induced oxidative renal injury in rats. Arch Med Res 2006;37:822–829
6. Leonard SS, Xia C, Jiang BH, et al. Resveratrol scavenges reactive oxygen species and effects radical-induced cellular responses. Biochem Biophys Res Commun 2003;309:1017–1026
7. Pervaiz S, Holme AL. Resveratrol: its biologic targets and functional activity. Antioxid Redox Signal 2009;11:2851–2897
8. Ceriello A. New insights on oxidative stress and diabetic complications may lead to a "causal" antioxidant therapy. Diabetes Care 2003;26:1589–1596
9. Nishikawa T, Edelstein D, Du XL, et al. Normalizing mitochondrial superoxide production blocks three pathways of hyperglycaemic damage. Nature 2000;404:787–790
10. MacMillan-Crow LA, Thompson JA. Tyrosine modifications and inactivation of active site manganese superoxide dismutase mutant (Y34F) by peroxynitrite. Arch Biochem Biophys 1999;366:82–88
11. Kim JA, Wei Y, Sowers JR. Role of mitochondrial dysfunction in insulin resistance. Circ Res 2008;102:401–414
12. Baur JA, Pearson KJ, Price NL, et al. Resveratrol improves health and survival of mice on a high-calorie diet. Nature 2006;444:337–342
13. Lagouge M, Argmann C, Gerhart-Hines Z, et al. Resveratrol improves mitochondrial function and protects against metabolic disease by activating SIRT1 and PGC-1alpha. Cell 2006;127:1109–1122
14. Um JH, Park SJ, Kang H, et al. AMP-activated protein kinase-deficient mice are resistant to the metabolic effects of resveratrol. Diabetes 2010;59:554–563
15. Liang F, Kume S, Koya D. SIRT1 and insulin resistance. Nat Rev Endocrinol 2009;5:367–373
16. Perez-de-Arce K, Foncea R, Leighton F. Reactive oxygen species mediates homocysteine-induced mitochondrial biogenesis in human endothelial cells: modulation by antioxidants. Biochem Biophys Res Commun 2005;338:1103–1109
17. Suematsu N, Tsutsui H, Wen J, et al. Oxidative stress mediates tumor necrosis factor-alpha-induced mitochondrial DNA damage and dysfunction in cardiac myocytes. Circulation 2003;107:1418–1423
18. Liu CS, Tsai CS, Kuo CL, et al. Oxidative stress-related alteration of the copy number of mitochondrial DNA in human leukocytes. Free Radic Res 2003;37:1307–1317
19. Heddi A, Stepien G, Benke PJ, Wallace DC. Coordinate induction of energy gene expression in tissues of mitochondrial disease patients. J Biol Chem 1999;274:22968–22976
20. Shen X, Zheng S, Thongboonkerd V, et al. Cardiac mitochondrial damage and biogenesis in a chronic model of type 1 diabetes. Am J Physiol Endocrinol Metab 2004;287:E896–E905
21. Koya D, Haneda M, Nakagawa H, et al. Amelioration of accelerated diabetic mesangial expansion by treatment with a PKC beta inhibitor in diabetic db/db mice, a rodent model for type 2 diabetes. FASEB J 2000;14:439–447
22. Deji N, Kume S, Araki S, et al. Structural and functional changes in the kidneys of high-fat diet-induced obese mice. Am J Physiol Renal Physiol 2009;296:F118–F126
23. Kume S, Uzu T, Horiike K, et al. Calorie restriction enhances cell adaptation to hypoxia through Sirt1-dependent mitochondrial autophagy in mouse aged kidney. J Clin Invest 2010;120:1043–1055
24. Kakoki M, Kizer CM, Yi X, et al. Senescence-associated phenotypes in Akita diabetic mice are enhanced by absence of bradykinin B2 receptors. J Clin Invest 2006;116:1302–1309
25. Daiber A, Oelze M, August M, et al. Detection of superoxide and peroxynitrite in model systems and mitochondria by the luminol analogue L-012. Free Radic Res 2004;38:259–269
26. Guo W, Adachi T, Matsui R, et al. Quantitative assessment of tyrosine nitration of manganese superoxide dismutase in angiotensin II-infused rat kidney. Am J Physiol Heart Circ Physiol 2003;285:H1396–H1403
27. Takaya K, Koya D, Isono M, et al. Involvement of ERK pathway in albumin-induced MCP-1 expression in mouse proximal tubular cells. Am J Physiol Renal Physiol 2003;284:F1037–F1045
28. Kume S, Haneda M, Kanasaki K, et al. SIRT1 inhibits transforming growth factor beta-induced apoptosis in glomerular mesangial cells via Smad7 deacetylation. J Biol Chem 2007;282:151–158
29. Kim SY, Jeoung NH, Oh CJ, et al. Activation of NAD(P)H:quinone oxidoreductase 1 prevents arterial restenosis by suppressing vascular smooth muscle cell proliferation. Circ Res 2009;104:842–850
30. Civitarese AE, Ukropcova B, Carling S, et al. Role of adiponectin in human skeletal muscle bioenergetics. Cell Metab 2006;4:75–87
31. Ha H, Lee HB. Reactive oxygen species as glucose signaling molecules in mesangial cells cultured under high glucose. Kidney Int Suppl 2000;77:S19–S25
32. Iglesias-De La Cruz MC, Ruiz-Torres P, Alcamí J, et al. Hydrogen peroxide increases extracellular matrix mRNA through TGF-beta in human mesangial cells. Kidney Int 2001;59:87–95
33. Kakimoto M, Inoguchi T, Sonta T, et al. Accumulation of 8-hydroxy-2′-deoxyguanosine and mitochondrial DNA deletion in kidney of diabetic rats. Diabetes 2002;51:1588–1595
34. Kiritoshi S, Nishikawa T, Sonoda K, et al. Reactive oxygen species from mitochondria induce cyclooxygenase-2 gene expression in human mesangial cells: potential role in diabetic nephropathy. Diabetes 2003;52:2570–2577
35. Munusamy S, MacMillan-Crow LA. Mitochondrial superoxide plays a crucial role in the development of mitochondrial dysfunction during high glucose exposure in rat renal proximal tubular cells. Free Radic Biol Med 2009;46:1149–1157
36. Kowluru RA, Atasi L, Ho YS. Role of mitochondrial superoxide dismutase in the development of diabetic retinopathy. Invest Ophthalmol Vis Sci 2006;47:1594–1599
37. Shen X, Zheng S, Metreveli NS, Epstein PN. Protection of cardiac mitochondria by overexpression of MnSOD reduces diabetic cardiomyopathy. Diabetes 2006;55:798–805
38. Williams MD, Van Remmen H, Conrad CC, Huang TT, Epstein CJ, Richardson A. Increased oxidative damage is correlated to altered mitochondrial function in heterozygous manganese superoxide dismutase knockout mice. J Biol Chem 1998;273:28510–28515
39. Rodriguez-Iturbe B, Sepassi L, Quiroz Y, Ni Z, Wallace DC, Vaziri ND. Association of mitochondrial SOD deficiency with salt-sensitive hypertension and accelerated renal senescence. J Appl Physiol 2007;102:255–260
40. van der Loo B, Labugger R, Skepper JN, et al. Enhanced peroxynitrite formation is associated with vascular aging. J Exp Med 2000;192:1731–1744
41. Cruthirds DL, Novak L, Akhi KM, Sanders PW, Thompson JA, MacMillan-Crow LA. Mitochondrial targets of oxidative stress during renal ischemia/reperfusion. Arch Biochem Biophys 2003;412:27–33
42. MacMillan-Crow LA, Crow JP, Kerby JD, Beckman JS, Thompson JA. Nitration and inactivation of manganese superoxide dismutase in chronic rejection of human renal allografts. Proc Natl Acad Sci USA 1996;93:11853–11858
43. Milne JC, Lambert PD, Schenk S, et al. Small molecule activators of SIRT1 as therapeutics for the treatment of type 2 diabetes. Nature 2007;450:712–716